

99.997%), S(SiMe₃)₂, technical grade (90%) trioctylphosphine oxide (TOPO), technical grade trioctylphosphine (TOP, 90%), and anhydrous toluene (99.8%). Tetradecylphosphonic acid (TDPA, 98%) was obtained from Alfa Aesar. Methanol (99.9%) and acetone (99.7%) were purchased from Fisher and used as received.

Synthesis

Under flowing argon, in a 250 mL 3-neck flask, equipped with a septum, a thermometer adapter, and a gas adapter, TOPO (3.77 g, 9.0 mmol), TDPA (0.22 g, 7.0 mmol), and 0.4 mmol of the desired Cd precursor (CdO: 0.05 g; Cd(OAc)₂: 0.09 g) were mixed. This Cd solution was then heated to 320 °C with stirring. In a glovebox, a chalcogenide stock solution was prepared by mixing TOP (2.0 g, 5.0 mmol), anhydrous toluene (~0.1 g), and 0.6 mmoles of the desired chalcogenide: (i) 0.11 g (S(SiMe₃)₂), (ii) 0.05 g (Se), or (iii) 0.08 g (Te). The chalcogenide stock solution was drawn into a syringe (3 mL) in the glovebox, transferred to the Schlenk line, and then rapidly injected (~1.0 s) into the heated Cd solution. After the appropriate time (15 s–7200 s), the reaction vessel was placed into a boiling water bath. Once the reaction mixture reached ~60 °C, the reaction was quenched *via* the addition of a previously prepared 50 : 50 methanol/acetone solution.

Optical characterization

UV-VIS absorption spectra were collected at room temperature on a Varian Carey 400 spectrophotometer. Each aliquot was quenched directly in a UV cell containing toluene. The spectra were collected from 800 to 300 nm with a scan rate of 0.5 nm per minute.

Transmission electron microscopy

An aliquot of the desired solution was placed directly onto a carbon coated copper TEM grid (300 mesh) purchased from Electron Microscopy Sciences. The aliquot was then allowed to dry overnight. The resultant particles were studied using a Philips CM 30 TEM operating at 300 kV accelerating voltage.

Powder X-ray diffraction

The powder X-ray diffraction (XRD) patterns of the CdE nanocrystals were obtained on a Siemens 5D500 diffractometer using Cu K α radiation, excited at 45 kV and 30 mA. The X-rays were collimated at the source with 1 degree divergence scatter slits. The detector had 1 degree scatter and receiving slits.

Results and discussion

This temporal study was undertaken to elucidate the controlled crystal growth of CdE through the pyrolysis of CdO and Cd(OAc)₂. Three fundamental parameters were unvaried: (i) the ratio of cadmium precursor (CdO or Cd(OAc)₂) to surfactants (TDPA/TOPO); (ii) the moles of chalcogenide injected; and (iii) the temperature of the reaction over a 7200 s time period. It should be noted that although the cadmium precursor was varied, both CdO and Cd(OAc)₂ resulted in nanocrystals of similar shape and size under identical reaction conditions. For the sake of brevity, the UV-VIS spectra and TEM images presented herein are derived solely from reactions with the CdO precursor. The exciton peak of the absorption spectrum for each aliquot was recorded at various time intervals and the results are listed in Tables 1, 2, and 3 for CdS, CdSe, and CdTe, respectively.

CdE nanoparticles were prepared by slight modification to a method recently investigated by Peng and coworkers.⁴⁷ Experimentally, TOPO, TDPA, and a cadmium precursor were heated to 320 °C under Ar flow until a transparent solution

Table 1 UV-VIS absorption data for CdS nanospheres

Reaction time/s	$\lambda_{\text{max}}/\text{nm}$
15	436
25	438
60	441
660	444
3600	446

Table 2 UV-VIS absorption data for CdSe nanorods

Reaction time/s	Length/nm	Aspect ratio (<i>c</i> : <i>a</i>)	$\lambda_{\text{max}}/\text{nm}$
15	10.8 (0.5)	3 : 1	549
25	^a	^a	572
35	^a	^a	580
60	21.5 (1.5)	6.4 : 1	587
120	24 (2.1)	6.8 : 1	597
360	^a	^a	617
660	32.5 (5.8)	3.6 : 1	624
3600	^a	^a	636
7200	25.7 (5.7)	2.3 : 1	651

^aTEM images not obtained.

Table 3 UV-VIS absorption data CdTe tetrapods

Reaction time/s	$\lambda_{\text{max}}/\text{nm}$
15	589
35	640
60	663
120	684 ^a

^aSize of particles precluded obtaining a λ_{max} after this time.

resulted. A chalcogenide solution was then injected into the reaction vessel (Scheme 1). The growth temperature was then set to 320 °C. Aliquots were taken from the reaction vessel and quenched in toluene at time intervals of 15, 25, 35, 60, 120, 360, 660, 1800, 3600, and 7200 s. The progress of the crystal growth for each CdE was monitored by UV-VIS spectroscopy and TEM and the results obtained for CdS, CdSe, and CdTe are discussed individually, in detail, below.

Cadmium sulfide

For the synthesis of CdS, upon injection of the TOP/S(SiMe₃)₂ stock solution, the reaction mixture went from colorless to yellow over a 7200 s period. The UV-VIS spectra (Fig. 1) of aliquots taken from the reaction mixture exhibited little change over this time period. A shift in the exciton peak from 436 to 444 nm (Table 1) was observed and is consistent for TOP capped CdS nanocrystals of 4 to 5 nm in size.⁴⁸ In

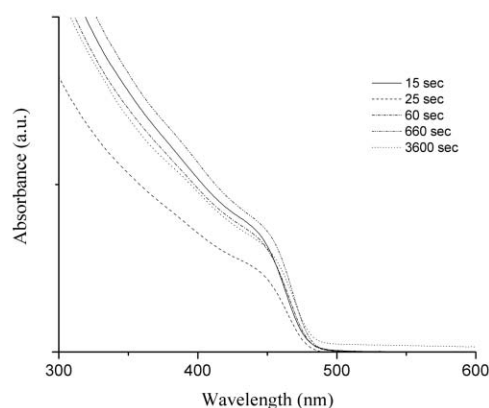


Fig. 1 UV-VIS spectra of CdS samples taken at intervals between 15 and 3600 s.

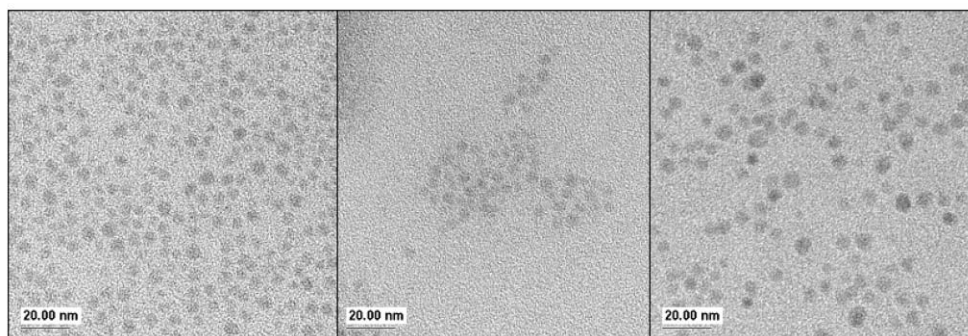


Fig. 2 From left to right, TEM images of CdS at (a) 15, (b) 660, and (c) 3600 s.

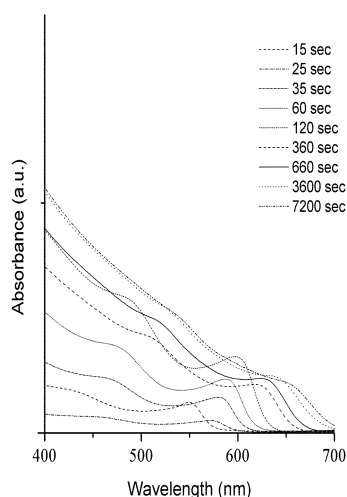


Fig. 3 UV-VIS spectra of CdSe nanorods taken at intervals between 15 and 7200 s.

confirmation, TEM images (Fig. 2) reveal little variation in spherical morphology *versus* time. The particles generally ranged from 4 to 5 nm in size, throughout the duration of the experiment. As found in similar syntheses, it seems that TDPA and tech grade TOPO are unable to facilitate anisotropic wurtzite growth of CdS under the reaction conditions presented. Therefore, CdS nanocrystals with a spherical shape are obtained. Powder X-ray diffraction was performed on the aliquot obtained at 7200 s and confirms the existence of a hexagonal greenockite phase (wurtzite type structure) with a mean crystallite diameter calculated from the Scherrer equation to be 3.7(5) nm.

Cadmium selenide

Under identical synthetic conditions to CdS nanoparticles, the cadmium reaction mixture changed from light yellow to wine red upon injection of the Se/TOP stock solution. Aliquots were taken over a 7200 s reaction time and the exciton peak of the

UV-VIS absorption spectra exhibited a systematic increase from 549 to 651 nm over this time period (Fig. 3, Table 2). To identify the morphology of the CdSe nanocrystals, TEM images (Fig. 4) were obtained for samples representative of various time intervals throughout the reaction. Surprisingly, instead of obtaining spherical particles analogous to CdS, CdSe exhibited rod shape morphologies. The presence of TDPA and tech grade TOPO facilitates anisotropic wurtzite growth of CdSe along the *c* axis, in effect generating the nanorods. Powder X-ray diffraction analysis for the aliquot obtained at 7200 s confirmed the cadmoselite phase of CdSe (a wurtzite type structure) with a mean crystallite diameter of 8.0 nm. It has been proposed that a highly acidic environment may influence this type of growth for CdSe *via* protonation of particular faces.³²

The rods grew from 10.8 by 3.6 nm (15 s aliquot) to a size of 25.7 by 11.2 nm (7200 s aliquot) with a small percentage of bipodal, tripodal, and tetrapodal morphologies present in each sample. The largest aspect ratio was observed at 120 s with a ratio of 6.8 : 1. At this aspect ratio, the spontaneous organization of single 24 by 3.5 nm CdSe nanorods into tracks over one micron in length was observed (Fig. 5). The tracks were produced when a drop of a toluene–nanorod dispersion air-dried on a carbon coated TEM grid. Typically, when CdSe nanorods are dried, they do so isotropically (see Fig. 4); therefore, if a solution containing rods is slowly deposited on a substrate, as the solution evaporates over time (*i.e.*, days) some ordering is observed.⁴⁹ However, the spontaneous organization of single CdSe nanorods into such long tracks shown in Fig. 5 has not been previously reported. The force believed to be capable of forming such long tracks of CdSe is typically attributed to dipole–dipole attraction between nanorods. The formation of long chains of CdTe quantum dots has been recently reported and their formation rationalized by dipole–dipole interaction.⁵⁰ A similar explanation would also account for the long tracks of CdSe nanorods observed here.

To relate the obtained UV-VIS spectra to the growth of nanorods, it should be noted that as the rod grows, the long axis (the *c* axis) grows beyond the quantum confinement

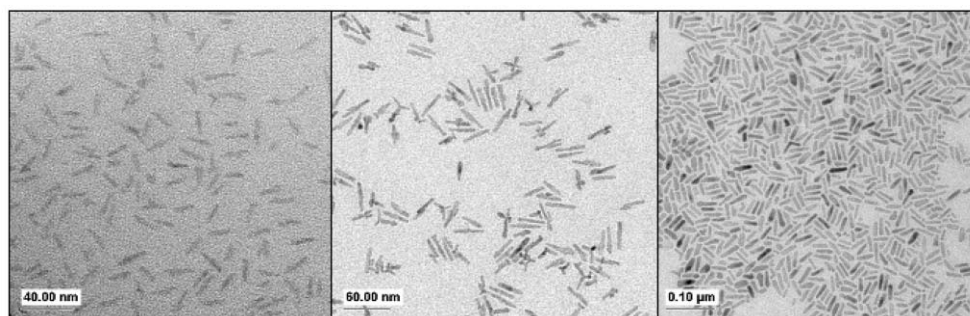


Fig. 4 From left to right, TEM images of CdSe nanorods at (a) 15, (b) 660, and (c) 7200 s.

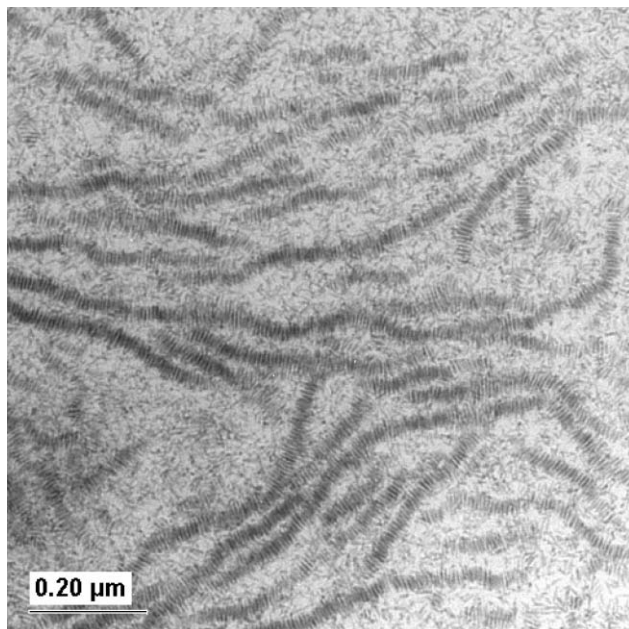


Fig. 5 Spontaneous organization of single 24 by 3.5 nm CdSe nanorods into tracks over one micron in length.

regime. Therefore, the red shift observed in the exciton peak is dependent only on the diameter of the short axis (a axis) of the rods. In this study, the a axis grew from 3.6 to 11.2 nm, consistent with the 549 to 651 nm shift in the exciton peak.³⁶

Cadmium telluride

With respect to the synthesis of CdTe nanocrystals, the reaction vessel charged with the cadmium precursor, tech grade TOPO, and TDPA changed from colorless to dark brown-red upon injection of the Te stock solution at 320 °C. The UV-VIS spectra revealed exciton peaks for aliquots taken within the first 360 s of the reaction (Fig. 6, Table 3). However, the absorption spectra were relatively featureless for the last 6240 s of the reaction indicating growth beyond the confinement regime for CdTe.

A TEM image of the nanocrystals obtained from the 15 s aliquot surprisingly revealed the presence of a tetrapod morphology (Fig. 7). Reports of tetrapods for CdSe and CdS synthesized by solution phase methods are available in the literature;^{7,32,51} however, this is the first published report of a tetrapod morphology for CdTe. ‡ Analogous to the synthesis of CdS and CdSe tetrapods, we rationalize that upon injection of the Te stock solution the reaction conditions favor the CdTe

‡A tetrapod morphology for CdTe was recently reported by X. G. Peng and coworkers at the 225th ACS National Meeting: March 23–27, 2003 New Orleans, Louisiana, USA.

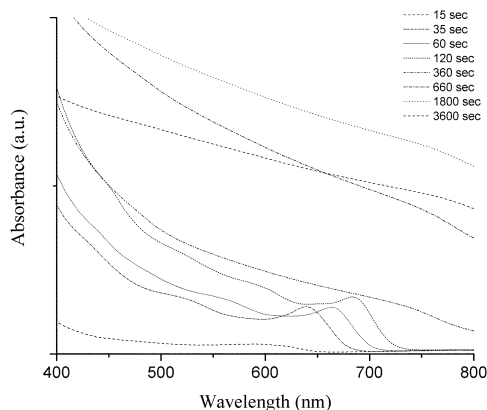


Fig. 6 UV-VIS spectra of CdTe samples taken at intervals between 15 and 3600 s.

clusters nucleating in a tetrahedron shaped zinc blende phase with four (111) faces equivalent to the (00 $\bar{1}$) face of the wurtzite structure. Therefore, as previously discussed for the growth of CdSe rods, if under acidic conditions wurtzite growth was favored for CdTe, one wurtzite arm would be generated from each face of the zinc blende tetrahedron; resulting in the production of a tetrapod morphology.^{7,25,32,51} The tetrapods at the 15 s interval have arms \sim 15 nm in length and are \sim 3.5 nm in diameter; consistent with the exciton peak observed in the absorption spectrum. After 7200 s of heating at 320 °C, a mixture of CdTe dots, rods and tetrapods on the order of 20 to 80 nm in size was generated due to Ostwald ripening and continued wurtzite growth. The XRD pattern of the CdTe sample was not sufficiently resolved to be able to determine the phase of the material isolated.

Conclusion

We have demonstrated that the controlled growth of CdE *via* the pyrolysis of CdO and Cd(OAc)₂, at the specific Cd to E mole ratio of 0.67 to 1, results in a spherical morphology for CdS, rod-like morphologies for CdSe, and tetrapod morphologies for CdTe. To our knowledge, this is the first time tracks of over a micron of self-assembled 3.5 by 24 nm sized CdSe nanorods have been observed. In addition, this is the first published report of a tetrapod morphology for CdTe. In conclusion, for the synthetic scheme previously described, we have elucidated the vastly different growth patterns and shapes of CdS, CdSe, and CdTe that form during the first 7200 s after injection of a chalcogenide solution using these alternative precursors. By simply controlling the reaction time, we can systematically generate specific structural types. Future work shall examine the detailed reaction conditions necessary to gain further control over resultant morphology.

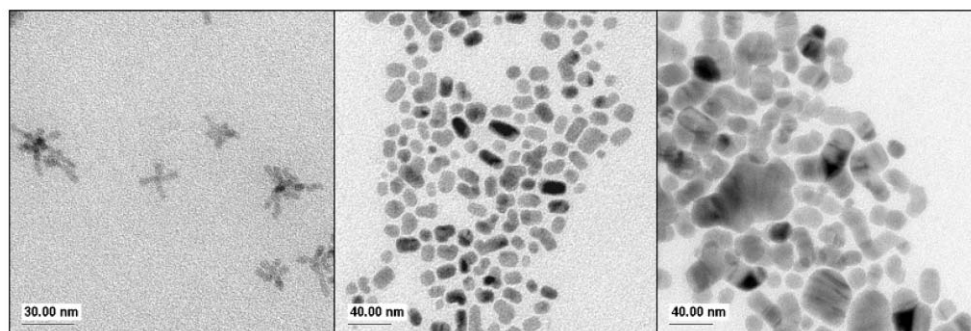


Fig. 7 From left to right, TEM images of CdTe samples taken at (a) 15, (b) 1660, and (c) 3600 s.

References

- 1 J. R. Heath, *Acc. Chem. Res.*, 1999, **32**.
- 2 A. P. Alivisatos, *Science*, 1996, **271**, 933.
- 3 H. Weller, *Adv. Mater.*, 1993, **5**, 88.
- 4 H. Weller, *Angew. Chem., Int. Ed. Engl.*, 1993, **32**, 41.
- 5 R. E. Smalley and B. I. Yakobson, *Solid State Commun.*, 1998, **107**, 597.
- 6 X. G. Peng, L. Manna, W. D. Yang, J. Wickham, E. Scher, A. Kadavanich and A. P. Alivisatos, *Nature*, 2000, **404**, 59.
- 7 L. Manna, E. C. Scher and A. P. Alivisatos, *J. Cluster Sci.*, 2002, **13**, 521.
- 8 J. R. Heath, *Science*, 1995, **270**, 1315.
- 9 C. Priester and M. Lannoo, *Phys. Rev. Lett.*, 1995, **75**, 93.
- 10 H. T. Jiang and J. Singh, *IEEE J. Quantum Electron.*, 1998, **34**, 1188.
- 11 Y. Ebiko, S. Muto, D. Suzuki, S. Itoh, K. Shiramine, T. Haga, Y. Nakata and N. Yokoyama, *Phys. Rev. Lett.*, 1998, **80**, 2650.
- 12 S. Fafard, Z. R. Wasilewski, C. N. Allen, D. Picard, M. Spanner, J. P. McCaffrey and P. G. Piva, *Phys. Rev. B: Condens. Matter*, 1999, **59**, 15368.
- 13 C. Heyn and C. Dumat, *J. Cryst. Growth*, 2001, **227**, 990.
- 14 M. Grundmann, J. Christen, N. N. Ledentsov, J. Bohrer, D. Bimberg, S. S. Ruvimov, P. Werner, U. Richter, U. Gosele, J. Heydenreich, V. M. Ustinov, A. Y. Egorov, A. E. Zhukov, P. S. Kopev and Z. I. Alferov, *Phys. Rev. Lett.*, 1995, **74**, 4043.
- 15 L. Landin, M. S. Miller, M. E. Pistol, C. E. Pryor and L. Samuelson, *Science*, 1998, **280**, 262.
- 16 N. L. Pickett, F. G. Riddell, D. F. Foster, D. J. Cole-Hamilton and J. R. Fryer, *J. Mater. Chem.*, 1997, **7**, 1855.
- 17 J. F. Wang, M. S. Gudiksen, X. F. Duan, Y. Cui and C. M. Lieber, *Science*, 2001, **293**, 1455.
- 18 J. T. Hu, L. S. Li, W. D. Yang, L. Manna, L. W. Wang and A. P. Alivisatos, *Science*, 2001, **292**, 2060.
- 19 M. P. Pileni, *Supramol. Sci.*, 1998, **5**, 321.
- 20 T. S. Ahmadi, Z. L. Wang, T. C. Green, A. Henglein and M. A. ElSayed, *Science*, 1996, **272**, 1924.
- 21 S. P. Wang, N. Mamedova, N. A. Kotov, W. Chen and J. Studer, *Nano Lett.*, 2002, **2**, 817.
- 22 W. C. W. Chan and S. M. Nie, *Science*, 1998, **281**, 2016.
- 23 M. Bruchez, M. Moronne, P. Gin, S. Weiss and A. P. Alivisatos, *Science*, 1998, **281**, 2013.
- 24 C. T. Black, C. B. Murray, R. L. Sandstrom and S. H. Sun, *Science*, 2000, **290**, 1131.
- 25 Y. W. Jun, Y. Y. Jung and J. Cheon, *J. Am. Chem. Soc.*, 2002, **124**, 615.
- 26 V. F. Puentes, K. M. Krishnan and A. P. Alivisatos, *Science*, 2001, **291**, 2115.
- 27 S. H. Sun and C. B. Murray, *J. Appl. Phys.*, 1999, **85**, 4325.
- 28 W. Huynh and A. P. Alivisatos, *Proc. Electrochem. Soc.*, 2001, **2001-10**, 195.
- 29 W. U. Huynh, J. J. Dittmer and A. P. Alivisatos, *Science*, 2002, **295**, 2425.
- 30 M. C. Schlamp, X. G. Peng and A. P. Alivisatos, *J. Appl. Phys.*, 1997, **82**, 5837.
- 31 H. Mattoussi, L. H. Radzilowski, B. O. Dabbousi, E. L. Thomas, M. G. Bawendi and M. F. Rubner, *J. Appl. Phys.*, 1998, **83**, 7965.
- 32 L. Manna, E. C. Scher and A. P. Alivisatos, *J. Am. Chem. Soc.*, 2000, **122**, 12700.
- 33 T. Vossmeier, L. Katsikas, M. Giersig, I. G. Popovic, K. Diesner, A. Chemseddine, A. Eychmuller and H. Weller, *J. Phys. Chem.*, 1994, **98**, 7665.
- 34 X. G. Peng, J. Wickham and A. P. Alivisatos, *J. Am. Chem. Soc.*, 1998, **120**, 5343.
- 35 D. Battaglia and X. G. Peng, *Nano Lett.*, 2002, **2**, 1027.
- 36 C. B. Murray, D. J. Norris and M. G. Bawendi, *J. Am. Chem. Soc.*, 1993, **115**, 8706.
- 37 C. B. Murray, M. Nirmal, D. J. Norris and M. G. Bawendi, *Z. Phys. D: At., Mol. Clusters*, 1993, **26**, S231.
- 38 C. B. Murray, C. R. Kagan and M. G. Bawendi, *Science*, 1995, **270**, 1335.
- 39 J. Hambrock, A. Birkner and R. A. Fischer, *J. Mater. Chem.*, 2001, **11**, 3197.
- 40 P. S. Nair, T. Radhakrishnan, N. Revaprasadu, G. A. Kolawole and P. O'Brien, *Chem. Commun.*, 2002, 564.
- 41 M. Lazell and P. O'Brien, *J. Mater. Chem.*, 1999, **9**, 1381.
- 42 M. Lazell, S. J. Norager, P. O'Brien and N. Revaprasadu, *Mater. Sci. Eng. C*, 2001, **16**, 129.
- 43 P. Nair, T. Radhakrishnan, N. Revaprasadu, G. Kolawole and P. O'Brien, *Chem. Commun.*, 2002, 564.
- 44 L. H. Qu, Z. A. Peng and X. G. Peng, *Nano Lett.*, 2001, **1**, 333.
- 45 X. G. Peng, *Chem. Eur. J.*, 2002, **8**, 335.
- 46 Z. A. Peng and X. G. Peng, *J. Am. Chem. Soc.*, 2002, **124**, 3343.
- 47 Z. A. Peng and X. G. Peng, *J. Am. Chem. Soc.*, 2001, **123**, 183.
- 48 N. Myung, Z. F. Ding and A. J. Bard, *Nano Lett.*, 2002, **2**, 1315.
- 49 L. Li, J. Walda, L. Manna and A. Alivisatos, *Nano Lett.*, 2002, **2**, 557.
- 50 Z. Tang, N. A. Kotov and M. Giersig, *Science*, 2002, **297**, 237.
- 51 M. Chen, Y. Xie, J. Lu, Y. J. Xiong, S. Y. Zhang, Y. T. Qian and X. M. Liu, *J. Mater. Chem.*, 2002, **12**, 748.